Polymer 50 (2009) 3031–3036

Contents lists available at ScienceDirect

Polymer

journal homepage: www.elsevier.com/locate/polymer

Preparation and photocatalysis of TiO_2–fluoropolymer electrospun fiber nanocomposites

Tieshi He, Zhengfa Zhou, Weibing Xu*, Fengmei Ren, Haihong Ma, Jin Wang

Department of Polymer Science and Engineering, Hefei University of Technology, Hefei, 230009, China

ARTICLE INFO

Article history:
Received 14 December 2008
Received in revised form
17 March 2009
Accepted 14 April 2009
Available online 21 April 2009

Keywords:
Polymer composites
Titanium dioxide
Fluoropolymer fiber

ABSTRACT

The preparation and photocatalytic properties of titanium dioxide (TiO_2)–fluoropolymer fiber nanocomposites were studied. The fluoropolymer nanofibers with carboxyl group were prepared by electrospinning. The complex was formed between carboxyl on fluoropolymer electrospun fiber surface and titanium ion, and then the TiO_2 nanoparticles were immobilized on the surface of fluoropolymer electrospun fibers through hydrothermal complex-precipitation. By controlling the reaction conditions, different sizes and numbers of TiO_2 nanocrystals can be obtained. The Fourier transform infrared spectroscopy (FTIR) and X-ray photoelectron spectroscopy (XPS) results reveal that an interaction exists between TiO_2 and fluoropolymer fibers. The degradation of methylene blue solution is performed by TiO_2–fluoropolymer fiber nanocomposites under UV irradiation. There may be an adsorption–migration–photodegradation process during the degradation of methylene blue by using TiO_2–fluoropolymer fiber nanocomposites as photocatalyst. The experimental results show that the TiO_2–fluoropolymer fiber nanocomposites have good photocatalytic ability, recycling and stability for the potential applicability in an environmental remediation.

1. Introduction

TiO_2 as a semiconductor photocatalyst possesses high photocatalytic efficiency, complete decomposition and ease of preparation [1–3], and offers the potential complete mineralization of hazardous wastes and toxic water pollutants [4]. There are many methods for the preparation of TiO_2 [5]. The preparation of TiO_2 by hydrothermal synthesis can get high purity and perfect nanocrystal under mild conditions at reasonable cost with environmental friendship [6]. However, the TiO_2 nanocrystals are easily to agglomerate intrinsically, thus limiting their large scale application in waste water photocatalytic degradation. In order to solve the problem, semiconductor nanocrystals are successfully immobilized on inorganic porous carriers including silica [7], zeolite [8], and stainless steel [9], etc. The immobilization can prevent semiconductor nanocrystals from agglomeration and make it easy to reclaim from reaction mixtures at high yields. The fluoropolymers such as poly(vinylidene difluoride) have excellent weather, radiate, chemical and thermal resistance due to C–F bond on the main chain, and are suitable for catalyst carriers [10–12]. The fluoropolymer fiber mats from electrospinning comprised random nonwoven mesh of fibers with high surface areas, and were usually used as the catalyst carrier to improve the catalytic activities, efficiency of light utilization, and the flexibility in operation [13].

In this paper, TiO_2–fluoropolymer fiber nanocomposites were prepared. The photocatalytic activity and stability were investigated through degradation of methylene blue by using TiO_2–fluoropolymer fiber nanocomposites as photocatalyst under UV irradiation. The results show that the as-prepared nanomaterials have excellent photocatalytic activity and stability.

2. Experimental section

2.1. Materials

Titanium oxo-sulphate ($TiOSO_4$) was purchased from Zhonghe Chemical Plant, Dandong in China. Trifluoroethyl acrylate (TFA) was obtained from Xuejia Fluorine-silicon Chemical Co., Ltd, Harbin in China. Anatase Degussa P25 was purchased from Shanghai Haiyi Scientific & Trading Co., Ltd. Poly(vinylidene difluoride) (PVDF), methacrylic acid (MAA), methylene blue, urea and other chemicals were purchased from Shanghai Chemicals Ltd., and used as received.

2.2. Characterization

Perkin Elmer Spectrum 100 FTIR spectrometer was used to widely scan the synthetic products. JSM-6700F scanning electron microscopy

* Corresponding author. Tel./fax: +86 551 2901455.
E-mail address: xwb105105@sina.com (W. Xu).

0032-3861/$ – see front matter © 2009 Elsevier Ltd. All rights reserved.
doi:10.1016/j.polymer.2009.04.015

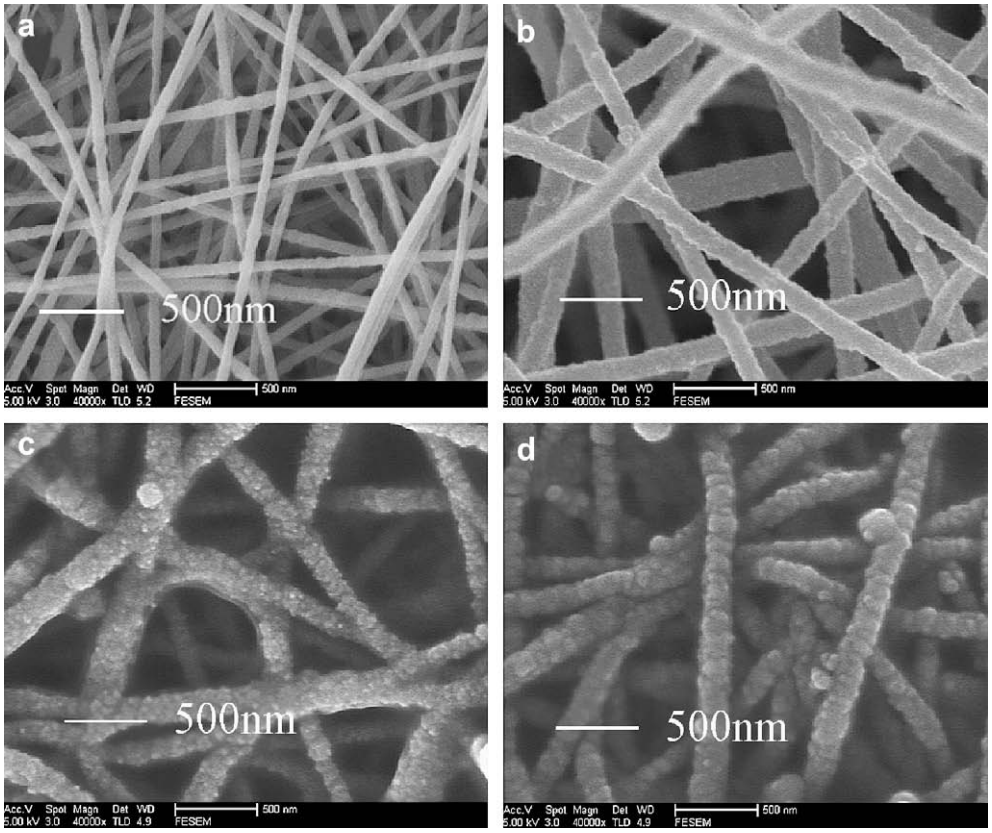

Fig. 1. SEM images of (a) poly (MAA-*co*-TFA)/PVDF electrospun fiber mats and TiO_2–fluoropolymer fiber nanocomposites prepared at 150 °C for (b) 3 h, (c) 6 h, (d) 12 h.

(SEM) was utilized to study the surface morphologies of the products. The specific surface area analyzed by ASAP 2020M + C. ESCALAB 250 X-ray photoelectron spectroscopy was used to study the structure of nanocomposites. High-resolution transmission electron microscope (HRTEM) image and the selected area electron diffraction (SAED) pattern were taken on JEOL 2010. The crystal structure was detected through the X-ray diffraction (XRD), Rigaku D/max-rB. The thermogravimetric analysis (TGA), Netzsch TG-209-F3, was applied to estimate the weight loss of composites. Ultraviolet–visible (UV/VIS) absorption spectra were obtained on a Shimadzu Solidspec-3700 DUV spectrophotometer at room temperature.

2.3. Preparation of poly(MAA-co-TFA)

The synthesis of MAA–TFA random copolymers was carried out using an automated reactor system. 30 g MAA, 70 g TFA, and 0.5 g 2,2-azobisisobutyronitrile (AIBN) were added into a 250 mL three-neck flask equipped with a condenser, a stirrer and a N_2 inlet. After polymerizing at 80 °C for 1 h, the reaction mixture was transferred to a stainless steel plate and placed in an oven at 40 °C for 12 h. Then the reaction mixture was maintained at 100 °C for 3 h to polymerize the remaining monomer.

2.4. Electrospinning

Poly(MAA-*co*-TFA)/PVDF electrospun fiber mats were prepared using a typical electrospinning process [14]. 10.3 g PVDF and 1.7 g poly(MAA-*co*-TFA) were first dissolved in 88 g N,N-dimethylformamide (DMF). The solution was electrospun at 25 kV positive voltage, 15 cm working distance (the distance between the needle tip and the target), and 1.0 mL h^{-1} flow rate. The collection time was set to 2.0 h. All manipulations were carried out at room temperature. The electrospun fiber mats of fluoropolymers were cut into strips of dimension 2.0 cm × 2.0 cm for the following experiments.

2.5. Preparation of TiO_2–fluoropolymer fiber nanocomposites

The above-mentioned strip of fluoropolymer electrospun fiber mats were immersed into 2.0 mL, 0.2 mol L^{-1} aqueous solution of titanium oxo-sulphate and 1.0 mL concentrated sulfuric acid in

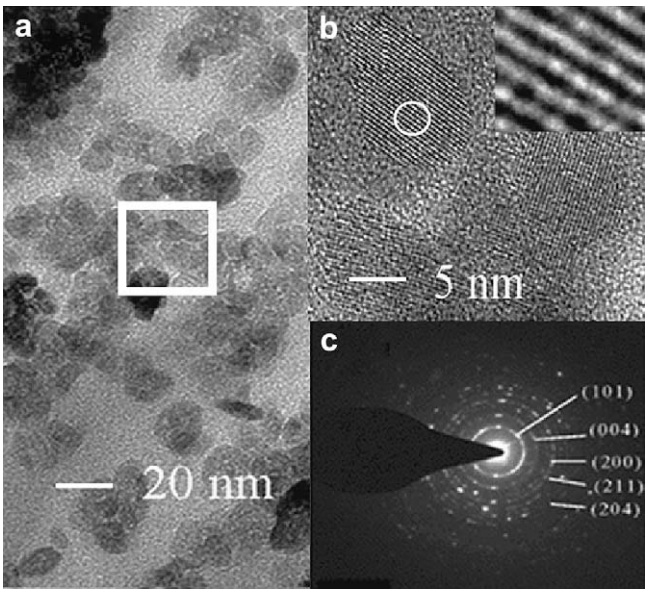

Fig. 2. HRTEM images of (a) TiO_2–fluoropolymer fiber nanocomposites prepared at 150 °C for 6 h, (b) enlarged image and (c) SAED of the sample.

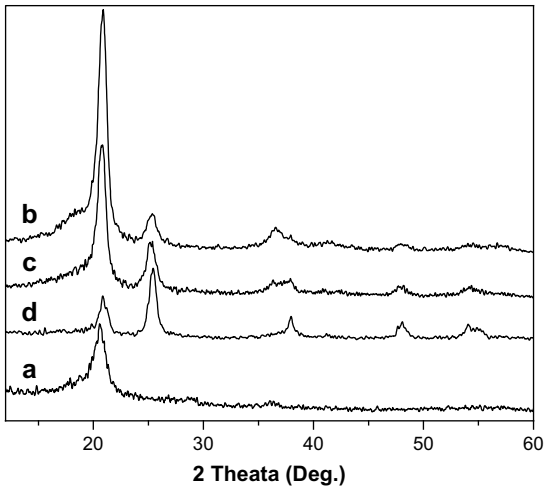

Fig. 3. XRD patterns of (a) poly(MAA-*co*-TFA)/PVDF electrospun fiber and the TiO_2–fluoropolymer fiber nanocomposites prepared at 150 °C for (b) 3 h, (c) 6 h, (d) 12 h.

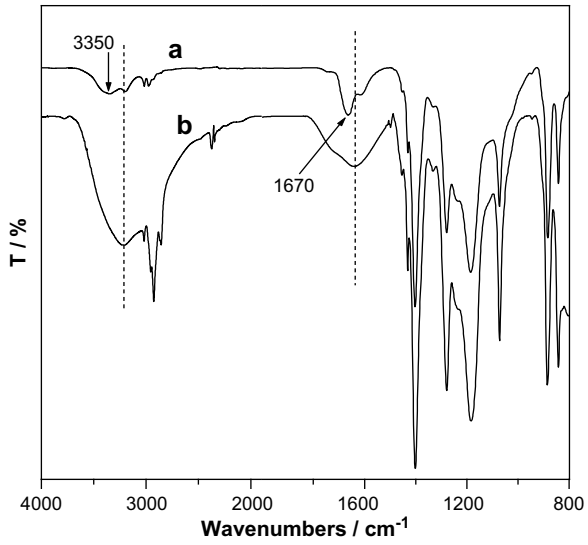

Fig. 4. FTIR spectra of (a) poly(MAA-*co*-TFA)-PVDF electrospun fiber mats, and (b) TiO_2–fluoropolymer fiber nanocomposites.

a 50 mL Teflon-lined stainless steel autoclave for 6 h in order to form the complex between carboxylic fluoropolymer electrospun fiber and titanium ion. Then 4.0 mL, 0.2 mol L^{-1} urea and 20 mL of distilled water were added. The autoclave was sealed at 150 °C for 3–12 h, and then cooled to room temperature. The TiO_2–fluoropolymer fiber nanocomposites were washed three times with distilled water under ultrasonic to remove the unreacted precursor and byproducts, and dried in vacuum at 80 °C for 12 h.

2.6. Photocatalytic activity

Photocatalytic degradation of methylene blue solution was performed by placing a 25 mL quartz tube in the middle of two 15 W shortwave UV lamps (254 nm) (Kexing Company, Changsha, China), the distance between two lamps is 15.0 cm. The UV lamp was positioned inside a cylindrical Pyrex vessel and surrounded by a circulating water jacket to remove the heat. The TiO_2–fluoropolymer nanocomposites and 15.0 mL, 16.0 mg L^{-1} methylene blue were added to the quartz tube. The TiO_2–fluoropolymer nanocomposites can be extended well in methylene blue solution without stirring. Prior to irradiation, the photocatalytic reaction system was stirred in a dark condition for 15 min to establish an adsorption–desorption equilibrium condition. The photocatalytic reaction system was sampled at regular intervals. The remaining methylene blue concentration after adsorption–desorption equilibrium (C_{in}) and during the photodegradation (C) was detected by UV/VIS at 665 nm. The degradation efficiency was expressed by (C/C_{in})%. The TiO_2 powder (Degussa P25) photocatalytic degradation of methylene blue was performed as stated in the previous steps with electromagnetic stirring, and the remaining methylene blue concentration was detected after the TiO_2 suspension was centrifuged.

3. Results and discussions

3.1. Morphology of TiO_2–fluoropolymer fiber nanocomposites

SEM image of the poly(MAA-*co*-TFA)/PVDF electrospun fiber mats is shown in Fig. 1(a). The poly(MAA-*co*-TFA)/PVDF electrospun fiber mats were made of random nonwoven mesh of fibers, and had an interconnected open porous structure.

TiO_2–fluoropolymer fiber nanocomposites prepared at 150 °C for different time are compared in Fig. 1(b)–(d). The almost spherical TiO_2 nanocrystals grow on the surface of poly(MAA-*co*-TFA)/PVDF electrospun fibers. The sizes and amount of TiO_2 nanoparticles increased with increasing reaction time, but the agglomeration of TiO_2 nanocrystals was also increased as reaction time prolonging.

3.2. Characterization of TiO_2–fluoropolymer nanocomposites

The HRTEM images of TiO_2–fluoropolymer fiber nanocomposites demonstrate the slightly agglomerated TiO_2 particles, shown in Fig. 2(a), which are inclusive of nanocrystallites with indistinct polygonal shape of about 10 nm in size as shown in Fig. 2(b). The selected area electron diffraction (SAED) pattern of anatase TiO_2 nanocrystallite is shown in Fig. 2(c), which is further discussed in the subsequent analysis using XRD in Fig. 3(b)–(d).

As shown in Fig. 3, the XRD patterns and the corresponding characteristic 2θ values of the diffraction peaks, it is confirmed that TiO_2 in as-prepared samples is identified as anatase-phase (ICDD PDF 21-1272) and the typical PVDF crystal structure [15]. No other polymorph of Titania is observed. Three intensity peaks only have appeared in the XRD patterns and all other high angle peaks have submerged in the background due to large line broadening. The broad diffraction peaks are attributed to the characteristic of small particle effect [16].

Typical FTIR spectra of poly(MAA-*co*-TFA)/PVDF electrospun fiber and TiO_2–fluoropolymer fiber nanocomposites are compared in Fig. 4. It is evident that the poly(MAA-*co*-TFA)/PVDF electrospun fiber mats have peaks at ~3350 cm^{-1} and ~1670 cm^{-1}, corresponding to a hydroxyl and a carbonyl stretching of the carboxyl groups present in poly(MAA-*co*-TFA). The corresponding hydroxyl and carbonyl absorption peaks of TiO_2–fluoropolymer fiber nanocomposites have been broadened and slightly shift to the low wavenumber. This may be due to that a complex existed between carboxyl on the surface of fluoropolymer electrospun fiber and titanic ion [17,18], and then the TiO_2 nuclei formed and grew into nanoparticles by hydrothermal precipitation.

The $Ti2p_{3/2}$ bonding energy is 458.7 and has 0.7 eV shift compared to the typical anatase TiO_2 (459.2 eV) [19], which resulted from the interaction between TiO_2 and fluoropolymer [20], shown in Fig. 5(a). As a result, the TiO_2 particles immobilized tightly on the surface of fluoropolymer nanofibers. There are peaks appeared at around 282.3 eV, 286.5 eV, 288.7 eV in the C_{1s} spectrum, shown in

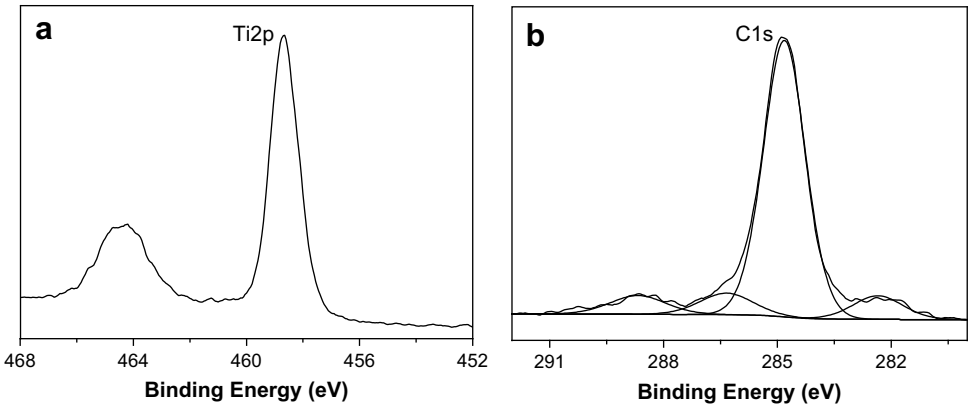

Fig. 5. XPS spectrum of TiO_2–fluoropolymer fiber nanocomposites prepared at 150 °C for 6 h.

Fig. 5(b). The peaks could be ascribed to the influence of carboxyl coordinated with titanic ion [21,22].

The TiO_2 content of TiO_2–fluoropolymer fiber nanocomposites is measured by TG, shown in Fig. 6. TG curve of poly(MAA-*co*-TFA)/PVDF electrospun fiber mats shows several thermal decomposition stages (Fig. 6(a)), but TiO_2–fluoropolymer fiber nanocomposites curves, shown in Fig. 6 (b)–(d), do not show thermal decomposition stage until 450 °C. This phenomenon may be due to that the low-molecular weight substances in poly(MAA-*co*-TFA)/PVDF electrospun fiber mats dissolved or crosslinked under long-time hydrothermal condition, and the interaction between TiO_2 and fluoropolymer may also improve the thermal stability of TiO_2–fluoropolymer fiber nanocomposites. The TiO_2 content of TiO_2–fluoropolymer fiber nanocomposites, which can be measured by the weight loss after fluoropolymer nanofiber was fully decomposed at 700 °C, was shown in Table 1.

UV/VIS spectra (Fig. 7) show the photosensitive properties of TiO_2–fluoropolymer fiber nanocomposites. As shown in Fig. 7(b), the UV/VIS absorption spectrum of the TiO_2–fluoropolymer fiber nanocomposites reflects the UV absorption band of the anatase TiO_2 nanocrystal [23], and the poly (MAA-*co*-TFA)/PVDF nanofiber mats have no evident absorption above 250 nm (Fig. 7(a)). This reveals that poly (MAA-*co*-TFA)/PVDF nanofiber mats do not disturb the light absorption of TiO_2 of TiO_2–fluoropolymer fiber nanocomposites during the photocatalytic reaction.

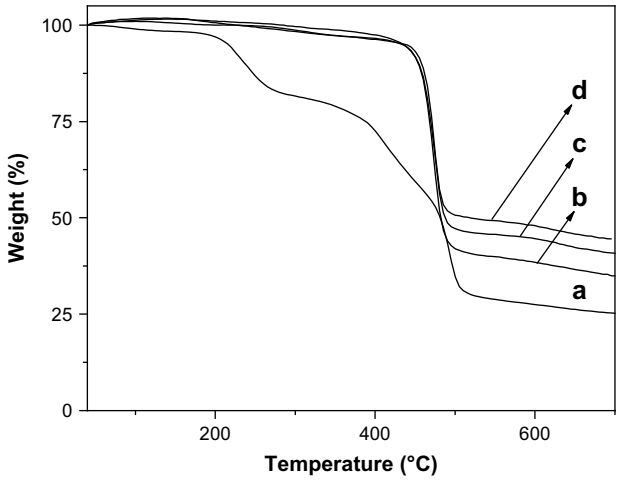

Fig. 6. Thermal gravity analytical of (a) poly(MAA-*co*-TFA)/PVDF electrospun fiber mats and TiO_2–fluoropolymer fiber nanocomposites prepared at 150 °C for (b) 3 h, (c) 6 h, (d) 12 h.

The specific surface area of Degussa P25 and poly(MAA-*co*-TFA)/PVDF electrospun fiber mats, and TiO_2–fluoropolymer fiber nanocomposites is shown in Table 2. The specific surface area of TiO_2–fluoropolymer nanocomposites is considerably higher than that of Degussa P25 and poly(MAA-*co*-TFA)/PVDF electrospun fiber mats. The specific surface area of TiO_2–fluoropolymer nanocomposites increases with increasing reaction time, but decreases when reaction time exceeds 6 h. This was due to that TiO_2 nanoparticles formed on the surface of poly(MAA-*co*-TFA)/PVDF electrospun fibers, but TiO_2 nanoparticles agglomerated seriously when reaction time exceeds 6 h, which was shown in Fig. 1.

3.3. Photocatalytic degradation of methylene blue

Photocatalytic ability of TiO_2–fluoropolymer fiber nanocomposites was investigated through photocatalytic degradation of methylene blue solution under UV irradiation. Fig. 8 shows the concentration changes of methylene blue in the presence of TiO_2–fluoropolymer fiber nanocomposites and other conditions under UV irradiation. In comparison, the experiments of blank sample, poly(MAA-*co*-TFA)/PVDF electrospun fiber mats and Degussa P25 were conducted for the methylene blue degradation under UV irradiation. Near-complete degradation of methylene blue occurred in 150 min in the presence of TiO_2–fluoropolymer fiber nanocomposites, shown in Fig. 8(c). A slight change in the methylene blue concentration was observed in the absence of a photocatalyst.

The remaining methylene blue is 0.05 wt.% after 150 min UV irradiation in the presence of TiO_2–fluoropolymer fiber nanocomposites prepared at 150 °C for 6 h (Fig. 8(c)). However, the remaining methylene blue is 46.72 wt.% in the presence of TiO_2 powders (Fig. 8(e)). The methylene blue degradation rate of TiO_2–fluoropolymer fiber nanocomposites is far higher than that of TiO_2 powder at the same or lower TiO_2 concentration, shown in Table 3. The main reason may be two. One was the specific surface area of TiO_2–fluoropolymer fiber nanocomposites was higher than that of TiO_2 powder (Table 2), another was the polymer fiber and the TiO_2 have some kind of synergistic effect.

Table 1
The TiO_2 content of TiO_2–fluoropolymer fiber nanocomposites prepared at 150 °C.

Sample		Weight loss (wt.%)	TiO_2 content (wt.%)
Poly(MAA-*co*-TFA)/PVDF electrospun fiber mats		−74.74	–
TiO_2–fluoropolymer fiber nanocomposites	3 h	−65.16	12.82
	6 h	−60.80	18.65
	12 h	−58.88	21.22

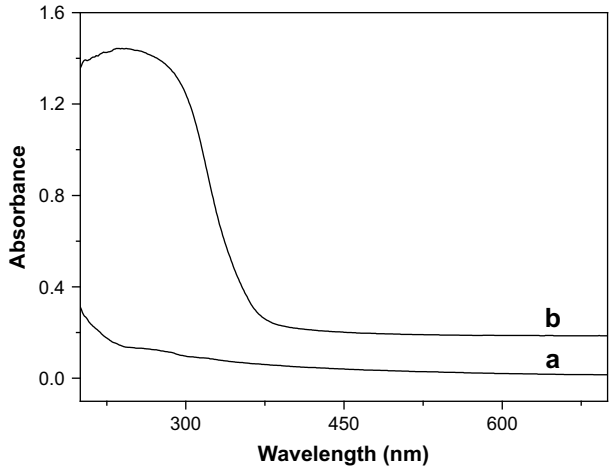

Fig. 7. UV/VIS absorption spectra of (a) poly (MAA-*co*-TFA)-PVDF electrospun fiber mats, (b) TiO_2–fluoropolymer fiber nanocomposites prepared at 150 °C for 6 h.

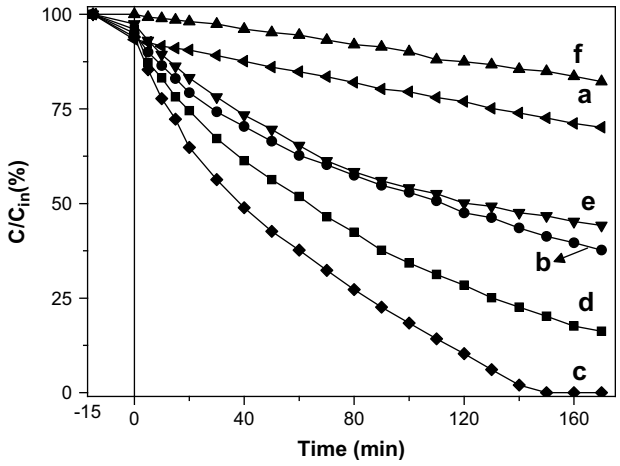

Fig. 8. Photocatalytic degradation of methylene blue by (a) poly(MAA-*co*-TFA)/PVDF electrospun fiber mats; TiO_2–fluoropolymer fiber nanocomposites prepared at 150 °C for (b) 3 h, (c) 6 h, (d) 12 h; (e) Degussa P25; and (f) blank sample.

In general, the methylene blue degradation rate of TiO_2–fluoropolymer fiber nanocomposites should increase with increasing the TiO_2 concentration. This was true in the system of TiO_2–fluoropolymer fiber nanocomposites prepared at 150 °C for 3 h and 6 h (Fig. 8(b) and (d), Table 3), but the methylene blue degradation rate of TiO_2–fluoropolymer fiber nanocomposites prepared at 150 °C for 6 h is considerably higher than that of TiO_2–fluoropolymer fiber nanocomposites prepared at 150 °C for 12 h (Fig. 8(c) and (d), Table 3). There may be an adsorption–migration–photodegradation process during the degradation of methylene blue by using TiO_2–fluoropolymer fiber nanocomposites as photocatalyst under UV irradiation. In the adsorption–migration–photodegradation process, methylene blue was first adsorbed by fluoropolymer nanofibers, then migrated to TiO_2 nanoparticles, and finally degraded by TiO_2 catalyst under UV irradiation. The adsorption effect of fluoropolymer nanofibers is obvious, but the TiO_2 concentration is considerably low when the preparation time of TiO_2–fluoropolymer fiber nanocomposites at 150 °C is less than 6 h. As a result, the methylene blue degradation rate of TiO_2–fluoropolymer fiber nanocomposites increased with increasing the TiO_2 concentration. The TiO_2 concentration is high, but the adsorption effect of fluoropolymer nanofibers decrease with decreasing of the surface area of fluoropolymer nanofibers, which can be observed in Fig. 1(d), when the preparation time of TiO_2–fluoropolymer fiber nanocomposites at 150 °C exceeds 6 h. As a result, the methylene blue degradation rate of TiO_2–fluoropolymer fiber nanocomposites decreased with increasing the TiO_2 concentration. The specific surface area data in Table 2 are in accordance with the assumption. This assumption can also explain why the methylene blue degradation rate of TiO_2–fluoropolymer fiber nanocomposites is considerably higher than that of TiO_2 powder at the same or lower TiO_2 concentration.

The photocatalytic stability of the TiO_2–fluoropolymer fiber nanocomposites prepared at 150 °C for 6 h was evaluated by the degradation of methylene blue solution under 10 times of repeated UV irradiation for 2.0 h each. The remaining methylene blue changes from 11.4 wt.% after 1st UV irradiation to 28.8 wt.% after 2nd UV irradiation, and stabilizes at about 29.9 wt.% from 3rd time all the ways till 10th time. The increase of remaining methylene blue from

Table 2
Specific surface area

Sample		Specific surface area ($m^2 g^{-1}$)
Degussa P25		50.0
Poly(MAA-*co*-TFA)/PVDF electrospun fiber mats		37.2
TiO_2–fluoropolymer fiber nanocomposites	150 °C, 3 h	45.5
	150 °C, 6 h	82.4
	150 °C, 12 h	68.3

Table 3
The TiO_2 concentration of TiO_2–fluoropolymer fiber nanocomposites and TiO_2 powders in solution.

Sample		TiO_2 concentration ($mg L^{-1}$)
Degussa P25		18.3
Poly(MAA-*co*-TFA)/PVDF electrospun fiber mats		–
Blank sample		–
TiO_2–fluoropolymer fiber nanocomposites	150 °C, 3 h	9.8
	150 °C, 6 h	15.3
	150 °C, 12 h	18.0

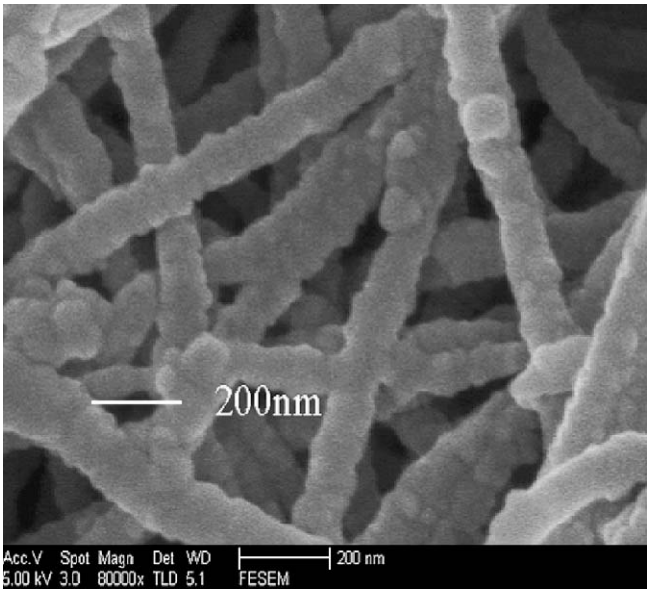

Fig. 9. SEM image of TiO_2–fluoropolymer fiber nanocomposites prepared at 150 °C for 6 h after 10 times degradation of methylene blue solution under UV irradiation for 2.0 h each.

1st time to 2nd time may be due to the absorption of methylene blue on the surface of electrospun fiber mats. Fig. 9 shows the SEM image of TiO_2–fluoropolymer fiber nanocomposites after 10 times degradation of methylene blue solution under UV irradiation for 2.0 h each, the TiO_2 particles are tightly immobilized on the surface of nanofibers after the degradation process, which indicates that TiO_2–fluoropolymer fiber nanocomposites possess high stability.

4. Conclusions

The carboxyl-containing fluoropolymer nanofiber mats with microporous are used as a template and prevent the agglomeration of TiO_2 nanoparticles in the process of the growth of TiO_2 on the fiber surface. By controlling the reaction conditions, different sizes and numbers of TiO_2 nanocrystals can be obtained. The FTIR and XPS results reveal that an interaction exists between TiO_2 and fluoropolymer fibers. The degradation results of methylene blue show that TiO_2–fluoropolymer fiber nanocomposites have good photocatalytic ability, recycling and stability under UV irradiation.

Acknowledgements

This work is supported by the National Natural Science Foundation of China (20776034), Doctoral Fund of Ministry of Education of China (20070359036).

References

[1] Zou Z, Ye J, Sayama K, Arakawa H. Nature 2001;414(6864):625–7.
[2] Liu Z, Sun DD, Guo P, Leckie JO. Nano Lett 2007;7(4):1081–5.
[3] Zhang J, Hu Y, Matsuoka M, Yamashita H, Minagawa M, Hidaka H, et al. J Phys Chem B 2001;105(35):8395–8.
[4] Ma J, Song W, Chen C, Ma W, Zhao J, Tang Y. Environ Sci Technol 2005;39(15):5810–5.
[5] Zou GF, Li H, Zhang YG, Xiong K, Qian YT. Nanotechnology 2006;17(11):S313–20.
[6] Stengl V, Bakardjieva S, Murafa N, Houskov V, Lang K. Microporous Mesoporous Mater 2008;110(2–3):370–8.
[7] Watthanaarun J, Supaphol P, Pavarajarn V. J Nanosci Nanotechnol 2007; 7(7):2443–50.
[8] Anandan S, Yoon M. J Photochem Photobiol C 2003;4(1):5–18.
[9] Yu JC, Ho W, Lin J, Yip H, Wong PK. Environ Sci Technol 2003;37(10):2296–301.
[10] Yee WA, Kotaki M, Liu Y, Lu X. Polymer 2007;48(2):512–21.
[11] Sopyan I, Watanabe M, Murasawa S, Hashimoto K, Fujishima A. J Electroanal Chem 1996;415(1–2):183–6.
[12] Zhang Z, Meng Q, Chung TCM. Polymer 2009;50(2):707–15.
[13] Choi SW, Jo SM, Lee WS, Kim YR. Adv Mater 2003;15(23):2027–32.
[14] Zhou ZF, He D, Xu WB, Ren FM, Qian YT. Mater Lett 2007;61(23–24):4500–3.
[15] Pan YV, Wesley RA, Luginbuhl R, Denton DD, Ratner BD. Biomacromolecules 2001;2(1):32–6.
[16] Luo ZP, Koo JH. Polymer 2008;49(7):1841–52.
[17] Drew C, Wang X, Bruno FF, Samuelson LA, Kumar J. Compos Interfaces 2005; 11(8–9):711–24.
[18] Graziola F, Girardi F, Bauer M, Di Maggio R, Rovezzi M, Bertagnolli H, et al. Polymer 2008;49(20):4332–43.
[19] Friedrich JF, Koprinarov I, Giebler R, Lippitz A, Unger WES. J Adhes 1999;71 (2-3):297–321.
[20] Kbushalani D, Ozin GA, Alex K. J Mater Chem 1999;9(7):1491–500.
[21] Sakthivel S, Kisch H. Angew Chem Int Ed 2003;42(40):4908–11.
[22] Dunuwila DD, Gagliardi CD, Berglund KA. Chem Mater 1994;6(9):1556–62.
[23] Yu XD, Wu QY, Jiang SC, Guo YH. Mater Charact 2006;57(4–5):333–41.